Cement & Concrete Composites 40 (2013) 40–47

Contents lists available at SciVerse ScienceDirect

Cement & Concrete Composites

journal homepage: www.elsevier.com/locate/cemconcomp

Non-saturated ion diffusion in concrete – A new approach to evaluate conductivity measurements

Nilla Olsson [a,b], Véronique Baroghel-Bouny [b], Lars-Olof Nilsson [a,*], Mickaël Thiery [b]

[a] Laboratory of Building Materials, Lund University, P.O. Box 118, SE-221 00 Lund, Sweden
[b] Materials Department, IFSTTAR, 4-20 Boulevard Newton Cité Descartes, Champs sur Marne, F-77447 Marne la Vallée Cedex 2, France

ARTICLE INFO

Article history:
Received 24 August 2012
Received in revised form 28 March 2013
Accepted 4 April 2013
Available online 11 April 2013

Keywords:
Ion transport
Non-saturation
Chloride
Alkali

ABSTRACT

Non-saturated ion diffusion properties of cementitious materials were evaluated in an experimental study. To assess these properties, resistivity measurements have been performed on mortars with different binders (ordinary Portland cement – OPC, OPC with 5% silica fume, 40% slag and 70% slag, respectively) and different water-to-binder ratios (w/b, 0.38 and 0.53). Specimens have been conditioned to eight different climates with relative humidity (RH) from 100% to 33% RH in order to assess an effective diffusion coefficient. The results from the resistivity measurements have been corrected for changes of the conductivity of the pore solution when drying to different degrees of saturation.

The diffusion coefficients for Portland cement binders within the range 100–59% RH are presented. They showed that the diffusion coefficient of the mortar with high w/b ratio was higher at high RH, but at low RH the opposite trend was found. By comparing these results with the corresponding desorption isotherms, it is shown that the diffusion coefficient for the two w/b ratios have the same dependency on the degree of saturation.

1. Introduction

Corrosion of the reinforcement is the major degradation mechanism for concrete structures and causes serious damage all over the world. The most common reasons for initiation of corrosion in concrete structures are carbonation and chloride ingress into the structure. Both these processes are strongly dependent on the transport properties of the material. Moisture conditions have a decisive effect on these transport properties [1].

All structures undergo variations in moisture distribution over time. Climate, with precipitation and often large temperature differences, is a major driving force for moisture transport, which causes differences in the concrete's moisture distribution. The fact that many structures are built with concrete with a low *w/b* ratio also makes self-desiccation a major contributor to moisture distribution variations. Self-desiccation is the reason why submerged structures may also undergo variations in moisture distribution over time [2,3].

No generally accepted method is available for estimating or for measuring ion transport properties in non-saturated conditions [4,5]. This is a problem when models are used for service-life design of concrete structures. For obtaining reliable and relevant results, these models need to consider the moisture dependency of chloride transport and other ion transport processes such as leaching. In this area, there is currently not sufficient knowledge to make accurate predictions of the service-life of concrete structures. There is also a lot of work to be done for understanding the link between transport properties and microstructure [6].

The phenomenon of non-saturated ion transport has been investigated in different ways. Several studies, for example Guimaraes et al. [7] and Climent et al. [8], have used Fick's second law and determined chloride diffusion coefficients from obtained profiles in non-saturated specimens. Guimaraes et al. used sodium chloride crystals to apply the chlorides. Climent et al. have used a gaseous source of chloride to avoid disturbing the specimen's conditioning. Vera et al. [9] and Nielsen and Geiker [10] have in the same way used Fick's second law, but these studies have included effects of binding of chlorides. Vera et al. have used the same procedure as Climent et al. Nielsen and Geiker used a NaCl solution and then quickly dried the samples to the same weight as before exposure.

Buchwald [11] and Francy [12] have both used impedance spectroscopy and the Nernst–Einstein equation for evaluating the chloride diffusion coefficient. Buchwald discusses how different masonry materials show a different behaviour with a decreasing degree of saturation. Francy's aim is to model transport, and he concludes that it is crucial to divide the moisture accurately into one part that contributes to ion transport and one part that does

* Corresponding author. Tel.: +46 46 222 7408; fax: +46 46 222 4427.
E-mail address: lars-olof.nilsson@byggtek.lth.se (L.-O. Nilsson).

0958-9465/$ - see front matter © 2013 Elsevier Ltd. All rights reserved.
http://dx.doi.org/10.1016/j.cemconcomp.2013.04.001

Table 1
Equivalent conductivity at infinite solution, λ_i^0 and conductivity coefficients G_i at 25 °C.

Ionic species	λ_i^0 (cm^2 S/mol)	G_i (mol/l)$^{-0.5}$
OH^-	198.0	0.353
Na^+	50.1	0.733
K^+	73.5	0.584

not. Otherwise the results can be very misleading. This has also been shown in a modelling study by Nilsson [13].

In the present work, the effect of moisture content on the diffusion of ions in non-saturated cementitious systems is investigated. The electrical resistivities of mortar samples conditioned to relative humilities from 100% to 33% RH are measured. For the OPC-mortars, the Nernst–Einstein equation is used to calculate the chloride diffusion coefficients from these measurements, after correcting the resistivity for changing ion concentrations in the pore solution after drying.

The effects of moisture content on the convective transport (sorption) of ions are not included in this study.

2. Theory

Ionic diffusion may be compared with electrolytic conduction, as both represent a random walk of a charged species. The movement is caused by different mechanisms and driven by concentration gradients and electrical potential differences, respectively. This is the basis for the Nernst–Einstein equation, which was used in this study for evaluating the diffusion transport properties of cementitious materials.

2.1. The Nernst–Einstein equation

The Nernst–Einstein equation relates the conductivity of a bulk material σ (S/m) to the diffusion coefficient, D (m^2/s). The conductivity of the liquid phase σ_l, i.e. the pore solution, in porous materials is much greater than the conductivity of the solid and vapour phases, σ_s and σ_a respectively. Rajabipour [14], referred to by [15], showed that the contribution to the overall conductivity from the solid and vapour phases, is negligible. Pore solutions are typically in the range of $\sigma_l \approx 1$–20 S/m, the solid phase $\sigma_s \approx 10^{-9}$ S/m and air $\sigma_a \approx 10^{-15}$ S/m. The Nernst–Einstein equation is given in the following equation

$$\frac{\sigma}{\sigma_0} = \frac{D}{D_0} \tag{1}$$

where σ_0 (S/m) and D_0 (m^2/s) are the conductivity and the diffusion coefficient of the substance through the liquid phase of the material. For chloride ions, D_0 equals 1.483–1.484 $\times 10^{-9}$ m^2/s in electrolytes within the range 0.1–1.0 mol/l [16]. The calculated diffusion coefficient does not include any interaction of the ions with the binder. Atkinson and Nickerson [17] have compared the results on the ionic transport properties from conductivity and diffusion measurements and found good agreement at saturated conditions.

The ionic diffusion takes place in the liquid phase in the material. Therefore, it is interesting to compare ionic transport properties, how moisture is fixed to the material and what characteristics there are of moisture fixation at different RH ranges. During drying, part of the liquid phase is lost. Due to the pore connectivity and shape of the pores, the connectivity of the liquid phase is decreased. The connectivity of the liquid phase, i.e. pore solution, has been shown to be the factor that has the most significant effect on the conductivity of a porous material [15,18], naturally along with the volume of the pore solution (solution-filled porosity).

2.2. Conductivity of the pore solution

A key point contributing to obtaining accurate results of these measurements is having an accurate value for the conductivity of the liquid phase in the material [19]. The conductivity has been calculated from Eq. (2) and the chemical composition of the pore solution.

$$\sigma_{calc} = \sum_{i=1}^{n} c_i z_i \lambda_i \tag{2}$$

where c_i (mol/l) is the concentration, z_i (–) is the charge and λ_i (cm^2 S/mol) is the equivalent conductivity for ion i. This last parameter is a function of the equivalent conductivity at infinite dilution, λ_i^0, and the ion mobility, which is also dependent on the ionic strength of the solution [20].

The main contributors to the ionic strength of a pore solution in an OPC binder are the hydroxide and alkali ions. This have been shown both by measurements and modelling by Lothenbach and Winnefeld [21] and Snyder et al. [22]. Snyder et al. have also shown that the conductivity of the pore solution can be estimated from these ions. They have developed a single parameter method to calculate the pore solution conductivity for cementitious materials for concentrations up to 2 mol/l, but then with fairly high errors at concentrations above 1 mol/l. Their method has also been used, and verified with measurements, by Rajabipour and Weiss [15]. According to Snyder et al. the equivalent conductivity is calculated by using in the following equation:

$$\lambda_i = \frac{\lambda_i^0}{1 + G_i\sqrt{I_m}} \tag{3}$$

where G_i (mol/l)$^{-0.5}$ is an empirical coefficient for the electrical conductivity of solutions at various concentrations. The values of G_i are given in Table 1 [22]. In this table, values of λ_i^0 (cm^2 S/mol) [16] are also given. I_m is the effective molar ionic strength (mol/l water) and is calculated by:

$$I_m = \frac{1}{2}\sum_{i=1}^{n} m_i z_i^2 \tag{4}$$

where mi is the molarity (mol/l water) and z_i as in Eq. (2).

2.3. Concentration of hydroxides and alkalis

The concentration of hydroxide and alkali ions were calculated by using a method by Taylor [23]. This requires the chemical composition of the OPC, the mix proportions, the porosity and the degree of hydration for the different minerals in the cement. Then the total amount of alkali, $n_{Na,total}$ and $n_{K,\ total}$ (mol) is calculated by the following equation:

$$n_{Na,total} = 2\frac{C\varphi_{Na2O}}{M_{Na2O}} \tag{5}$$

where C (g) is the mass of cement, φ_{Na2O} (–) is the mass fraction of Na_2O (equivalent for K_2O) in the OPC and M_{Na2O} (g/mol) is the molar mass of Na_2O (equivalent for K_2O). The released alkali, $n_{Na,released}$ and $n_{K,\ released}$ (mol), is then calculated from the alkalis immediately released to the pore solution from highly soluble sulphate salts, and the alkalis continuously released during hydration from the different clinker phases, see the following equation:

$$n_{Na,released} = f_{Na,sulfate} n_{Na,total} + (1 - f_{Na,sulfate}) n_{Na,total}\left(\sum_i g_{Na,i}\alpha_i\varphi_i\right) \tag{6}$$

where $f_{Na,sulphate}$ (–) is the fraction of Na in the form of sulphates (this will vary from cement to cement, but $f_{Na,sulfates} = 0.35$ and

$f_{K,sulphate}$ = 0.55 according to Pollitt and Brown [24]), $g_{Na,i}$ is the mass fraction of the non-sulfate alkalis in clinker phase i, α_i (–) and φ_i (–) are the degree of hydration and the mass fraction of the same clinker phase. The values for $g_{Na,i}$ are given by Taylor [23]. In this study so far, the degree of hydration has been assumed similar for the different clinker phases, although the belite likely is less reacted than the other phases in the OPC system [25,26].

The released alkalis are then partly adsorbed on the solid phases in the paste and the main part of the adsorption in an OPC paste is on the C–S–H gel [23,27,28]. This also agrees with the findings of Brouwers and van Eijk [29]. Taylor [23], Hong and Glasser [27] and Stade [30] have found distribution ratios R_d, for the partition of alkalis between the solid phases in the paste and the pore solution. For a fixed Ca:Si ratio of the C–S–H, these distribution ratios are independent of the concentration in the pore solution. Moreover, Chen and Brouwers [31] have found a similar dependence for sodium, but a nonlinear dependence for potassium. Here, the method by Chen and Brouwers has been used, since the variation in concentration will be fairly high due to the decreased amount of pore solution during drying. Their range of studied concentrations is larger than what has been studied by Taylor, and Hong and Glasser. Stade studied adsorption at higher temperatures.

The concentration of sodium, [Na^+] (mol/l) is then calculated by:

$$[Na^+] = \frac{n_{Na,released}}{V_w + m_{C-S-H} R_{d,Na}} \quad (7)$$

where V_w (l) is the volume of pore solution, R_d (l/g) is the distribution ratio which is 0.45 l/g [31] and m_{C-S-H} (g) is the mass of C–S–H according to the following equation [32]:

$$m_{C-S-H} = \alpha m_{OPC} \left(\sum_i \frac{M_{C-S-H} \varphi_i}{M_i} \right) \quad (8)$$

where m_{OPC} is the mass of cement (g), M_{C-S-H} is the molar mass of C–S–H (g/mol), which is assumed to have an average composition of $C_{1.7}SH_4$ for the OPC binders, φ_i and M_i are the mass fraction (–) and the molar mass of the alite and belite in the OPC (g/mol) [32], one mole of either alite or belite leading to the formation of one mole of C–S–H.

The concentration of potassium, [K^+] (mol/l) is calculated by solving the equation [31]:

$$[K^+]V_w + 0.20[K^+]^{0.24} V_w m_{C-S-H} = n_{K,released} \quad (9)$$

where V_w, m_{C-S-H}, and $n_{K,released}$ are calculated for a basis of 100 g OPC when using Eq. (9). Finally the concentration of hydroxide ions is calculated as the sum of the sodium and potassium ions [23].

3. Methods

The conductivity of a material is the inverse of its resistivity. For each material and RH, the resistance was measured with direct current and with one electrode covering each side of the sample. To get as little effect as possible from temperature effects, the measurements were performed in a room maintained at 21.5 ± 0.5 °C. The effect of temperature on resistivity measurements has been reported by Polder [33]. This varies with moisture content and is approximately 3% and 5%/K on a saturated and a dry specimen, respectively. Polder also found that coefficients of variation of 10% are good, and 20% are normal for resistivity measurements.

To ensure electrical contact over the whole surface, a humid (damp) sponge was used. A systematic decrease in resistance was observed when making several measurements on the same specimen; the resistance decreased 6% as an average for three measurements. This could be caused by absorption of moisture in the part of the specimen closest to the sponge, and then a decrease in resistivity due to the increase of the volume of pore solution. To minimize this effect, only the first measurement was included in the results [34].

No method was found for estimating the changes in pore solution composition after drying to reach non-saturated conditions and no direct measurements on samples were found in literature. To estimate the effect of the increasing conductivity of the pore solution because of drying, the volume of water acting as a solute for the ions has been deduced from the degree of saturation of the samples. A similar approach has been used by Rajabipour and Weiss [15], but not using the same methods for calculating the resulting concentrations.

The degree of saturation, S, has been calculated as the mass ratio of water at the different RH and the water lost during the drying of water-cured specimens at 105 °C. Depending on the fixation mechanism, moisture is more or less strongly bound to the material, and then also more or less likely to participate in ionic transport. The water that has reacted with cement during hydration is chemically bound in the solid parts of the material and is unlikely to take part. At the other end of the range, there is free water in the largest capillary pores where ion diffusion can take place. Between those extremes, there is interlayer water between the C–S–H layers in the gel, and also adsorbed water on the solid walls in all pores in the material. Adsorbed water is more or less bound, depending on how far from the solid surface it is and then also how large the pore is [35].

To verify the calculated conductivities, six synthetic solutions were prepared and their conductivity was measured experimentally. The results from the synthetic solutions were 3–4% lower than the calculated conductivities, an acceptable agreement.

4. Materials

Eight mortars with four different binders were used in this study. The binders were ordinary Portland cement CEM I 42.5N (OPC), OPC with 5% silica fume, and OPC with 40% and 70% ground granulated blast furnace slag (slag), respectively (all by mass). The chemical compositions of the cement and the slag are given in Table 2. Two water/binder (w/b) ratios, 0.38 and 0.53, were used. The w/b ratio is calculated by using an equivalent volume ratio, i.e. the relation volume of paste to the volume of water, is constant for all binders. This gives a slight variation in w/b ratio for binders with slag and silica fume. A siliceous sand according to EN 196-1 was used as aggregate. For a detailed description of the composition of the mortars, see Table 3.

The mortars were cast as large blocks ($60 \times 25 \times 25$ cm^3), which were demoulded after one day and then put into containers with a limited amount of water (tap water) for wet curing. After one week, cores of 50 mm diameter were drilled horizontally from the blocks. The cores were immediately put back into their holes for further wet curing. The reason for keeping the samples in their blocks was to limit the volume of water, to reduce leaching as much as possible. After 2 months the cores, were cut into discs with thicknesses of 15 mm and 45 mm and again put back into their holes. The properties of the mortars are given in Table 4.

Conditioning the samples to different humidity started three months after casting. The samples were moved stepwise to drier and drier humidities to avoid surface cracking. There was a CO_2-absorbent in each climate box for minimizing the effects of carbonation. The humidities used at 20 °C were "100"%, 97.5%, 94%, 91%, 85%, 75%, 59%, and 33% RH. The humidity was maintained with saturated salt solutions [36]. During conditioning, the mass of each sample was determined to assess how much water had evaporated from the pore solution between the different RH stages. When the sample masses were stable, a mass change <0.02 g/week, some

Table 2
Composition of (a) the OPC and (b) the slag.

Chemical analysis XRF (g/100 g)		Mineralogical composition – XRD/Rietveld analysis (g/100 g)	
(*a*)			
SiO_2	19.88	Alite	66.66
Al_2O_3	4.47	Belite	8.42
Fe_2O_3	2.96	Aluminate	6.17
CaO	63.49	Ferrite	9.60
MgO	1.77	Arcanite	1.60
K_2O	0.858	Free Lime	0.06
Na_2O	0.169	Portlandite	0.47
TiO_2	0.318	Periclase	0.49
Mn_2O_3	0.046	Gypsum	1.17
P_2O_5	0.219	Hemihydrate	2.18
SrO	0.049	Calcite	3.11
Cl	0.028	Anhydrite	0.10
F	<0.1		
ZnO	0.015	Density	3035
Cr_2O_3	0.012	(kg/m^3)	
SO_3	2.96		
(*b*)			
SiO_2	36.11	Amorphous	96.67
Al_2O_3	9.87	Gypsum	2.34
Fe_2O_3	0.43	Anhydrite	0.17
CaO	42.25	Merwinite	0.82
MgO	7.26		
K_2O	0.41		
Na_2O	0.28		
TiO_2	0.61		
Mn_2O_3	0.35		
P_2O_5	0.01		
SrO	0.07		
BaO	0.08		
Cl	<0.005	Density	2917
F	<0.1	(kg/m^3)	
SO_3	3.3		

samples were moved to the next climate box with a lower RH. Three discs were conditioned for each mortar and in each climate.

The mass changes during conditioning have been used to determine the points for the specified RH on the desorption isotherm for the materials. The porosity after 14 months wet curing was determined from drying the samples at 105 °C. The density is assumed to be 1.00 g/cm^3 for all water evaporated from the samples. The volumes of the samples were determined from their masses in air and water after drying and vacuum saturation. At the same age, the non-steady state migration coefficient for chlorides was determined with the standardized method NT Build 492 [37]. The measured properties are given in Table 4.

5. Results and discussion

So far in this study, resistivity measurements have been performed on specimens for the specified climates, except 33% RH, where equilibrium is still not reached. Calculations of the pore solution conductivity have been done for the OPC binders. If not stated elsewhere, points in the graphs represent an average of the measurements on three specimens. The coefficient of variation varied between 4 % and 10 %.

5.1. Resistivity measurements

In Fig. 1, the conductivity relative to the conductivity at 100% RH is shown. From this figure, it is clear that there is a large drop in conductivity when going just below 100% RH. It can also be seen that for the specimens in equilibrium with 59% RH, all the mortars with the same w/b ratio show the same value of the relation σ/σ(100% RH). Between those two boundaries, however, there is a variation between the different binders. It seems that binders with slag have a steeper drop in conductivity. A detailed analysis of this will be performed after correction of the pore solution conductivity has been done. Another way of looking at the results is to express the conductivity as a function of the degree of saturation S, which is illustrated in Fig. 2. The difference between the different binders is smaller when the relative conductivity is related to the degree of saturation, S, compared to when it is related to RH.

In a model by Saetta et al. [38], a numerical relationship is used for the changes in diffusion coefficient with moisture content. This relationship includes h_c that is defined as the RH where the diffusion coefficient has lost half of its value. The study by Saetta et al. then evaluates the model by comparing it with experimental results for OPC binders. Even though some authors [9,10,39,40] have found good agreement with this model with h_c equal to 0.75 for OPC binders, a fixed value cannot be confirmed by this study. From Figs. 1 and 2, it seems to depend on binder composition and w/b ratio.

Fig. 3 shows the desorption isotherms and the conductivities of the mortars with w/b ratio 0.38. By comparing these two graphs, it can be seen that for all four binders, there is a relation between the moisture ratio in the material and its conductivity. For the contin-

Table 3
Composition of the mortars. Quantities are given in kg/m^3.

Cement/SCM	100/0	95/5	60/40	30/70	100/0	95/5	60/40	30/70
w/b	0.380	0.381	0.391	0.386	0.530	0.531	0.539	0.545
Cement	516	406	308	153	436	484	260	129
Slag	–	–	206	357	–	–	174	302
Silica fume	–	21	–	–	–	25	–	–
Water	196	204	198	200	231	239	234	235
Normsand	1548	1607	1543	1531	1525	1574	1519	1508
Plasticizer	1.18	1.06	0.94	0.96	–	–	–	–

Table 4
Properties of the mortars.

Cement/SCM	100/0	95/5	60/40	30/70	100/0	95/5	60/40	30/70
w/b	0.380	0.381	0.386	0.391	0.530	0.531	0.539	0.545
Plastic density (kg/m^3)	2256	2253	2236	2208	2198	2203	2199	2201
Air content (%)	6.4	6.0	6.5	6.9	6.1	6.0	5.7	5.0
Compressive strength at 28 days (MPa)	72.4	81.4	74.5	55.6	51.0	59.8	40.7	29.4
Porosity (%)	15	18	16	16	17	19	18	20
NT Build 492 D_{nssm} (10^{-12} m^2/s)	10.5	1.7	2.9	4.3	15.9	1.6	3.2	5.7

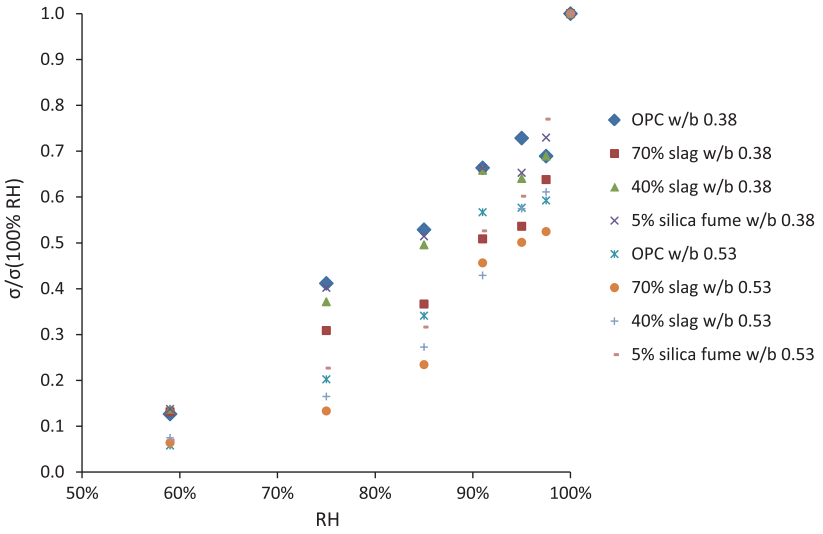

Fig. 1. All binders plotted, relative conductivity vs. RH.

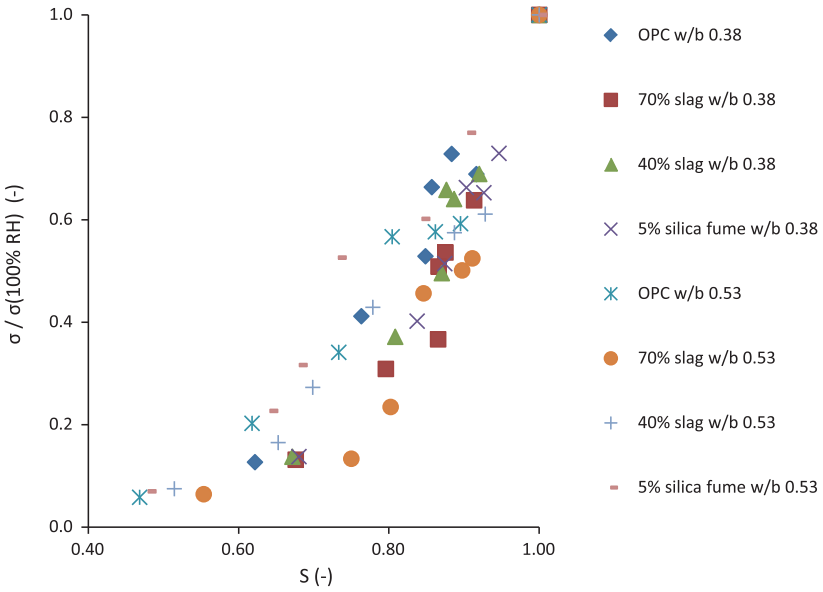

Fig. 2. The relative conductivity vs. degree of saturation.

ued evaluation of this, the pore solution conductivity needs to be taken into account.

The conductivities versus RH for the two w/b of all four mortars show a similar pattern. As seen in Fig. 4, the curves for the two w/b ratios intersect both for the overall conductivity and the desorption isotherm. At higher RH, diffusion in large capillary pores dominates the transport, and the mortar with higher w/b ratio has a larger transport. The mortar with the lower w/b ratio and larger amount of binder has more small capillary pores and gel pores, and at a certain point these pores dominate the transport and the diffusion in this material is larger. The intersection point is not similar in the different binders, and it is not possible to state its position before the correction of the pore solution composition is done.

5.2. Calculation of the chloride diffusion coefficient for the OPC binders

For the mortars with OPC binders, the pore solution composition, its conductivity and the chloride diffusion coefficient have been calculated at different degrees of saturation. To do this, the degree of hydration of the cement was assumed to be the same for all clinker phases, a simplification. Then the degree of hydration is so far assumed to be 0.7 for w/b ratio 0.38 and 0.9 for w/b 0.53. This is an estimation, which will be replaced by the results from the microstructural characterization later in this study.

All water that was lost during the drying phase at 105 °C is included in the calculation of the composition of the pore solution and the desorption isotherms. This gives an overestimation, since some of the chemically bound water is also lost at that high temperature [26], and this hard drying also induces micro cracks and changes the microstructure. Baroghel-Bouny [35] found a 13.5% difference when comparing drying at 105 °C with drying at room temperature with silica gel, which gives 3% RH. Much is known about moisture in cementitious materials, but it is still an open question as to what part acts as a solvent for the ions and what part is able to contribute to ion transport. The assumption about whether water acts as a solvent for the ions in this study will underestimate the increase in concentration of the pore solution during the drying process and overestimate the moisture ratio at the specified RHs.

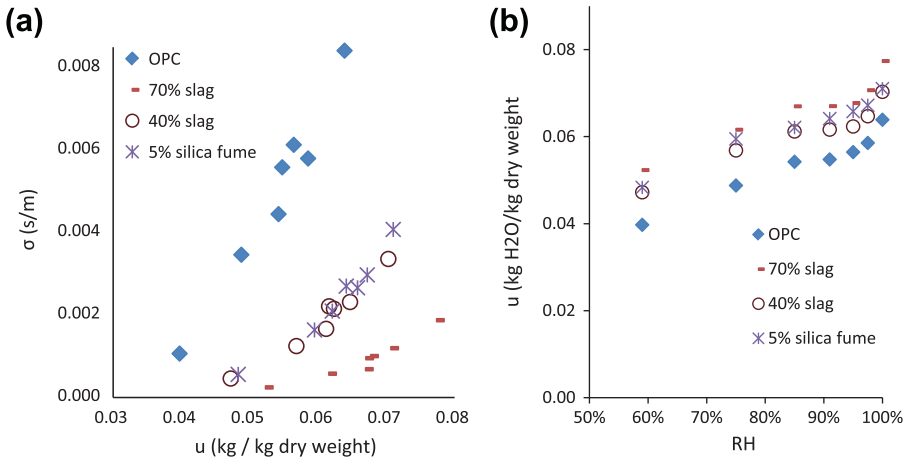

Fig. 3. (a) Results of resistivity measurements on mortars with w/b 0.38, as a function of moisture ratio. (b) The points on the desorption isotherm for the samples measured in a).

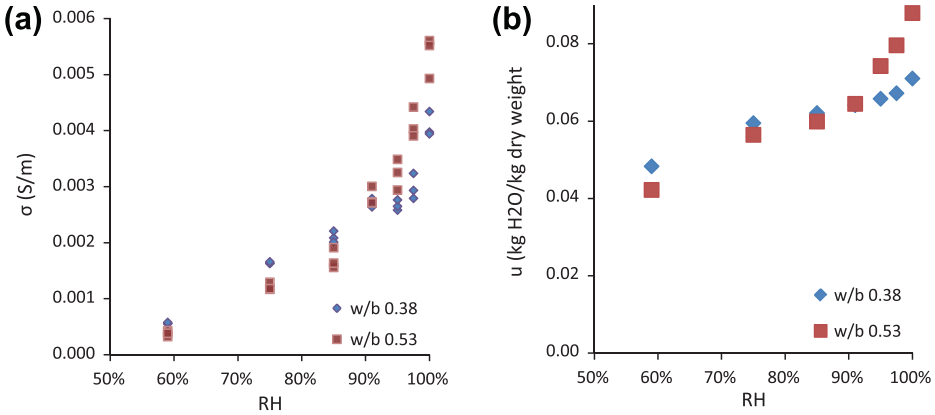

Fig. 4. (a) Results of resistivity measurements on mortars with OPC + 5% silica fume, as a function of RH. Each specimen is plotted as an individual point. (b) The points on the desorption isotherm for the samples measured in (a).

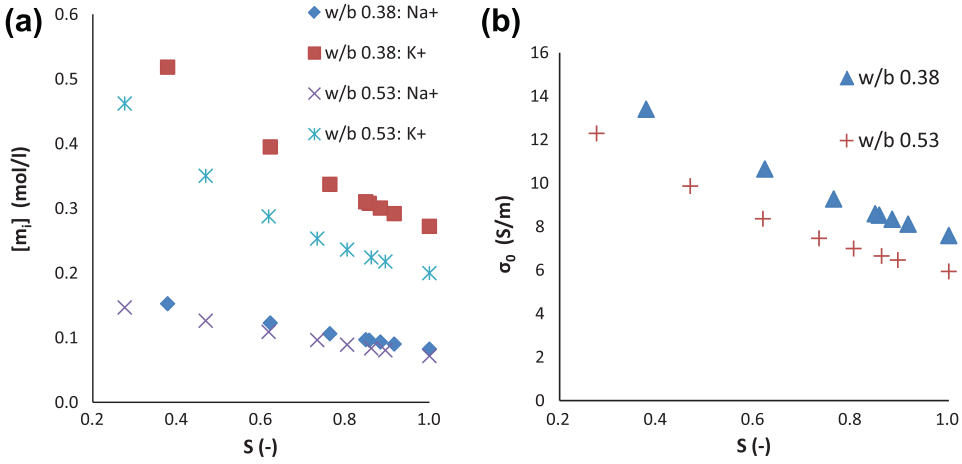

Fig. 5. (a) Calculated alkali concentrations depending on the degree of saturation. (b) Calculated conductivities of the pore solutions depending on the degree of saturation.

The decrease in RH may also affect the water content in the hydrates and here the primary interest is the C–S–H, which may affect the adsorption of alkalis. The stability of other solids may also be affected by the decreasing RH, which also may affect the composition of the pore solution [41,42].

The calculated alkali concentrations and conductivities are given in Fig. 5. The behaviour of the diffusion coefficient compared to the desorption isotherm was the same as for the conductivity, but with a slight change in the intersection point, as can be seen in Fig. 6.Baroghel-Bouny et al. [4] used the work by Francy [12]

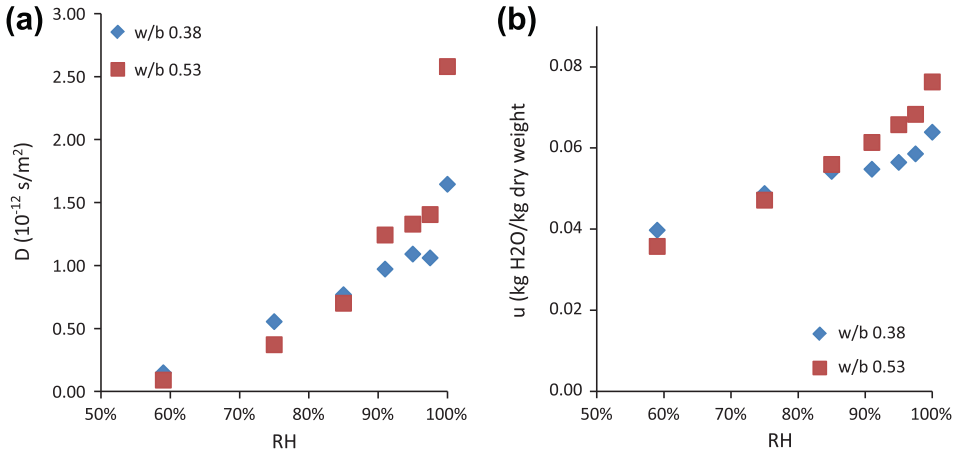

Fig. 6. (a) Calculated chloride diffusion coefficients for the OPC binders. (b) The points on the desorption isotherm for the samples measured in (a).

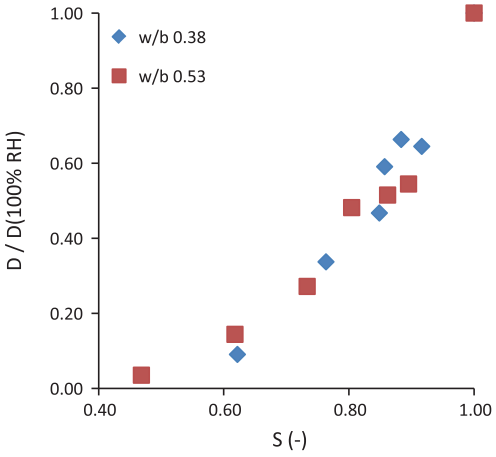

Fig. 7. Relative diffusion coefficient vs. degree of saturation for the OPC binders.

and assumed a similar behaviour for the diffusion coefficient for different w/b ratios. Buchwald [11] proposed a dependence on the degree of saturation S which has been used in the model by Baroghel-Bouny et al. as the relative chloride diffusion coefficient given in the following equation:

$$\frac{D_{Cl^-}(S)}{D_{Cl^-}(S=1)} = S^{\lambda} \tag{10}$$

From Francy's work, Baroghel-Bouny et al. have found $\lambda = 6$. Using the same relation on the results presented in Fig. 7 yields $\lambda = 4.5$. Francy also concluded that there does not seem to be any transport when the degree of saturation is lower than 0.50. The results in Fig. 7 show that at this level of saturation, the diffusion is only 4% of the value at saturation. Though, it should be pointed out that this is the result of three specimens from one binder composition.

The results in Fig. 7 also show that for this OPC, the w/b ratio does not affect the relation between the relative diffusion coefficient and the degree of saturation.

6. Conclusions

The results of this study confirm that the conductivity of the studied mortars is closely related to their desorption isotherms and the moisture content in each material. As expected, at high RH, the mortars with high w/b ratio have a higher conductivity than the mortars with low w/b ratio. When RH is decreasing, and the major transport paths in the large capillary pores are emptied, at some point, however, there is a shift and the mortars with low w/b ratio have higher conductivity. This is probably because there is more gel, and connected gel pores, in the mortars with lower w/b. From the results for the OPC binders, where the changes in pore solution concentration have been taken into account, it is clear that the variation of the diffusion coefficient with RH shows the same behaviour as the conductivity.

From the results from calculating the chloride diffusion coefficient for the OPC binders, it is shown that for this binder, the dependence of the relative diffusion coefficient on the degree of saturation is similar for the two water-binder ratios.

The available results can constitute major input data for models of chloride transport in non-saturated materials.

The study will be continued with calculations of the pore solution conductivity of the blended binders, and then a calculation of the chloride diffusion coefficients for the materials with those binders. Measurements on the specimens in equilibrium with 33% RH will be completed and included in the results. It can be expected from Fig. 4 that the diffusion coefficients will be near zero at this low RH.

Acknowledgements

The authors are grateful to NanoCem for the funding of the project, and to Bo Johansson and Jean-François Bouteloup for their kind help with the experiments.

References

[1] Neville A. Chloride attack of reinforced concrete: an overview. Matet Constr 1995;28:63–70.
[2] Nilsson L-O, Andersen A, Utgenannt TL. Chloride ingress data from field exposure in a Swedish road environment. Report P-00:5. Göteborg (Sweden): Department of Building Materials, Chalmers University of Technology; 2000.
[3] Tang L. A collection of chloride and moisture profiles from the träslövsläge field site – from 0.5 up to 10 years investigations. Report P-03:3. Göteborg (Sweden): Department of Building Materials, Chalmers University of Technology; 2003.
[4] Baroghel-Bouny V, Thiéry M, Wang X. Modelling of isothermal coupled moisture-ion transport in cementitious materials. Cem Concr Res 2011;41(8):828–41.
[5] Samson E, Marchand J, Snyder KA, Beaudoin JJ. Modeling ion and fluid transport in unsaturated cement systems in isothermal conditions. Cem Concr Res 2005;35(1):141–53.
[6] Glasser FP, Marchand J, Samson E. Durability of concrete – degradation phenomena involving detrimental chemical reactions. Cem Concr Res 2008;38:226–46.

[7] Guimarães ATC, Climent MA, Vera Gd, Vicente FJ, Rodrigues FT, Andrade C. Determination of chloride diffusivity through partially saturated Portland cement concrete by a simplified procedure. Constr Build Mater 2011;25(2):785–90.
[8] Climent MA, de Vera G, López JF, Viqueira E, Andrade C. A test method for measuring chloride diffusion coefficients through nonsaturated concrete: Part I. The instantaneous plane source diffusion case. Cem Concr Res 2002;32(7):1113–23.
[9] Vera Gd, Climent MA, Viqueira E, Antón C, Andrade C. A test method for measuring chloride diffusion coefficients through partially saturated concrete. Part II: The instantaneous plane source diffusion case with chloride binding consideration. Cem Concr Res 2007;37:714–24.
[10] Nielsen EP, Geiker MR. Chloride diffusion in partially saturated cementitious material. Cem Concr Res 2003;33:133–8.
[11] Buchwald A. Determination of the ion diffusion coefficient in moisture and salt loaded masonry materials by impedance spectroscopy. In: Proc third international Ph.D. symposium, Vienna, Austria; 2000.
[12] Francy O. Modélisation de la pénétration des ions chlorures dans les mortier partiellement saturés en eau. PhD. Toulouse: Univeristé Paul Sabatier; 1998.
[13] Nilsson L-O. A numerical model for combined diffusion and convection of chloride in non-saturated concrete. In: Second int RILEM workshop, testing and modelling chloride ingress into concrete, Paris; 2000.
[14] Rajabipour F. In situ electrical sensing and material health monitoring of concrete structures. PhD. Indiana: Purdue University; 2006.
[15] Rajabipour F, Weiss J. Electrical conductivity of drying cement paste. Mater Struct 2007;40(10):1143–60.
[16] Weast RC, editor. CRC handbook of chemistry and physics. Journal of the American Chemical Society. 56th ed. Washington (DC, USA): ACS; 1975.
[17] Atkinson A, Nickerson AK. The diffusion of ions through water-saturated cement. J Mater Sci 1984;19(9):3068–78.
[18] Chen W, Li Y, Shui Z. Percolation of phases in hydrating cement paste at early ages: an experimental and numerical study. In: Proc XIII ICCC, Madrid; 2011.
[19] Rajabipour F, Weiss J, Abraham D.M. Insitu electrical conductivity measurements to assess moisture and ionic transport in concrete. In: Advanced in concrete through science and engineering; proceedings of the international RILEM symposium. Evanston, Illinois; 2004.
[20] Bockris JOM, Reddy AKN. Modern Electrochemistry 1 Ionics. New York, Boston, Dordrecht, London, Moscow: Kluwer Academic Publishers; 2002. vol. 1.
[21] Lothenbach B, Winnefeld F. Thermodynamic modelling of the hydration of Portland cement. Cem Concr Res 2006;36(2):209–26.
[22] Snyder KA, Feng X, Keen BD, Mason TO. Estimating the electrical conductivity of cement paste pore solutions from OH−, K+ and Na+ concentrations. Cem Concr Res 2003;33(6):793–8.
[23] Taylor HFW. A method for predicting alkali ion concentrations in cement pore solutions. Adv Cem Res 1987;1:5–16.
[24] Pollitt HWW, Brown AW. The distribution of alkalis in Portland cement clinker. In: 5th ISCC. Tokyo: Cement Association of Japan; 1969.
[25] Kocaba V. Development and evaluation of methods to follow microstructural development of cementitious systems including slags. Lausanne: PhD, EPFL; 2009.
[26] Taylor HFW. Cement chemistry. London: Academic Press; 1990.
[27] Hong S-Y, Glasser FP. Alkali binding in cement pastes: Part I. The C–S–H phase. Cem Concr Res 1999;29(12):1893–903.
[28] Hong S-Y, Glasser FP. Alkali sorption by C–S–H and C–A–S–H gels: Part II. Role of alumina. Cem Concr Res 2002;32(7):1101–11.
[29] Brouwers HJH, vanEijk RJ. Alkali concentrations of pore solution in hydrating OPC. Cem Concr Res 2003;33(2):191–6.
[30] Stade H. On the reaction of C–S–H(di, poly) with alkali hydroxides. Cem Concr Res 1989;19(5):802–10.
[31] Chen W, Brouwers HJH. Alkali binding in hydrated Portland cement paste. Cem Concr Res 2010;40(5):716–22.
[32] Brouwers, H.J.H, VanEijk, R.J. Alkali concentrations of pore solution in hydrating OPC, Cem Concr Res 2003;33:191–6.
[33] Polder RB. Test methods for on site measurement of resistivity of concrete – a RILEM TC-154 technical recommendation. Constr Build Mater 2001;15:125–31.
[34] Andrade C, Alonso C, Arteaga A, Tanner P. Methodology based on the electrical resistivity for the calculation of reinforcement service life; metodologia basata sulla resistivita elettrica per la stima della vita di servizio delle armature metalliche nel calcestruzzo. Industria Italiana del Cemento 2001;71(Compendex):330–9.
[35] Baroghel-Bouny V. Water vapour sorption experiments on hardened cementitious materials: Part I: Essential tool for analysis of hygral behaviour and its relation to pore structure. Cem Concr Res 2007;37(3):414–37.
[36] Greenspan L. Humidity fixed points of binary aqueous solutions. J Res Mational Bureau of Standards – A, Phys Chem 1977;81A(1):89–96.
[37] NT Build 492. Concrete, mortar and cement-based materials: Chloride migration coefficient from non-steady state migration experiments, Nordtest. 1999.
[38] Saetta AV, Scotta RV, Vitaliani RV. Analysis of chloride diffusion into partially saturated concrete. ACI Mater J 1993;90:441–51.
[39] Bastidas-Arteaga E, Chateauneuf A, Sánchez-Silva M, Bressolette P, Schoefs F. A comprehensive probabilistic model of chloride ingress in unsaturated concrete. Eng Struct 2011;33(3):720–30.
[40] Ababneh A, Benboudjema F, Xi Y. Chloride penetration in nonsaturated concrete. J Mater Civ Eng 2003;15(GEOBASE):183–91.
[41] Albert B, Guy B, Damidot D. Water chemical potential: A key parameter to determine the thermodynamic stability of some hydrated cement phases in concrete? Cem Concr Res 2006;36(5):783–90.
[42] Lothenbach B. Thermodynamic equilibrium calculations in cementitious systems. Mater Struct 2010;43(10):1413–33.